RSC Advances

PAPER

View Article Online
View Journal | View Issue

Open Access Article. Published on 14 March 2018. Downloaded on 1/8/2025 8:54:51 PM.
This article is licensed under a Creative Commons Attribution-NonCommercial 3.0 Unported Licence.

Check for updates

Cite this: *RSC Adv.*, 2018, **8**, 10437

Cipadessains A–K, eleven limonoids from the fruits of *Cipadessa cinerascens*†

Dong-Mei Sun, Fa-Liang An, Shan-Shan Wei, Yan-Qiu Zhang, Xiao-Bing Wang, Jun Luo* and Ling-Yi Kong*

Received 24th January 2018
Accepted 26th February 2018

DOI: 10.1039/c8ra00728d

rsc.li/rsc-advances

Eleven new mexicanolide-type limonoids, cipadessains A–K (**1–11**), were isolated from the fruits of *Cipadessa cinerascens* (Pellegr) Hand.-Mazz. Their planar structures were determined based on IR, UV, 1D and 2D NMR spectra and HRESIMS data. The absolute configuration of **1** was elucidated by single-crystal X-ray diffraction using mirror Cu Kα radiation, and that of compounds **2–8** were determined by ECD analysis. Two mexicanolides bearing methoxybutenolide moiety originated from the furan ring **3** and **6**, showed significant cytotoxicity against HepG2 cell line with IC_{50} values of 5.23 ± 0.12, 8.67 ± 1.02 μM, respectively; and NO inhibitory activities in LPS-activated RAW 264.7 macrophages at nontoxic concentration (IC_{50} 5.79 ± 0.18, 6.93 ± 0.89 μM, respectively).

Introduction

Cipadessa cinerascens (Pellegr) Hand.-Mazz is a species of *Cipadessa* genus and known as 'Ya Luo Qing' or 'Lao Ya Fan' by the Dai.[1] Its roots and leaves have been used in Chinese folk medicine for the treatment of rheumatism, stomachache, dysentery, malaria, scald, and skin itch.[1–3] Previous reports demonstrated that terpenoids, flavonoids, steroids, and limonoids are the main bioactive constituents of *Cipadessa* genus.[2,3] Among those compounds, limonoids have become a point of interest in the field of natural products, because of its diverse skeletons (mexicanolides, methyl angolensates, trijugins, and cipadesins) and various biological effects such as cytotoxic, insecticidal, antioxidant, and trypanocidal activities.[2–6] Previous studies on *Cipadessa* genus focused on their leaves, roots, barks and stems.[4–15] To our knowledge, there have been few phytochemical investigations on the fruits of *Cipadessa* species. In continuing search for new bioactive limonoids, 11 new mexicanolide limonoids with various modified furan rings, cipadessains A–K (**1–11**), were isolated from the fruits of *C. cinerascens*. All the isolates were evaluated for NO inhibitory activities in LPS activated RAW 264.7 macrophages and cytotoxicity against HepG2 cell line. In this paper, we describe the isolation, identification of **1–11**, as well as their bioactivity screening.

State Key Laboratory of Natural Medicines, Department of Natural Medicinal Chemistry, China Pharmaceutical University, 24 Tong Jia Xiang, Nanjing 210009, People's Republic of China. E-mail: luojun1981ly@163.com; cpu_lykong@126.com; Fax: +86-25-8327-1405; Tel: +86-25-8327-1405

† Electronic supplementary information (ESI) available: HRESIMS, 1D and 2D NMR spectra of compounds **1–11** and ECD spectrum of **1–8** are available as supporting information. CCDC 1815118. For ESI and crystallographic data in CIF or other electronic format see DOI: 10.1039/c8ra00728d

Results and discussion

Cipadessain A (**1**), was isolated as white powder, and assigned to a molecular formula of $C_{32}H_{40}O_9$ on the basis of HRESIMS at *m/z* 591.2560 $[M + Na]^+$ (calcd $C_{32}H_{40}O_9Na$, 591.2565), corresponding with 13 degrees of unsaturation. Its IR absorption bands at 3460 and 1728 cm^{-1} showed the presence of hydroxyl and carbonyl functionalities. The NMR data (Table 1) revealed the characteristic resonances for β-substituted furan ring [δ_H 7.93 (H-21), 7.45 (H-23), and 6.50 (H-22), δ_C 143.4 (C-23), 142.4 (C-21), 120.5 (C-20), 109.7 (C-22)], four tertiary methyls (δ_H 1.42, 1.11, 0.85, 0.83); a characteristic downfield H-17 signal (δ_H 5.43); a ketone carbonyl (δ_C 217.3), three ester carbonyls (δ_C 175.1, 168.6, 167.2) and two unsaturated bonds (δ_H 6.90, 5.39; δ_C 139.6, 137.5, 127.6, 125.6). In the HMBC spectrum (Fig. 2), both angular methyls (C-28, C-29) were attached to C-4 (δ_C 38.7), were elucidated by the cross peaks from H_3-28 (δ_H 0.83) to C-29 (δ_C 20.3), C-5 (δ_C 41.8) and C-3 (δ_C 77.6), and from H_3-29 (δ_H 0.85) to C-28 (δ_C 22.9), C-5 (δ_C 41.8) and C-3 (δ_C 77.6); a C-6/7 esterificated appendage (δ_H 3.74; δ_C 52.3, 175.1) was easily verified by the HMBC cross peaks from H_2-6 (δ_H 2.98, 2.40) to C-5 (δ_C 41.8), C-7 (δ_C 175.1) and from OCH_3 (δ_H 3.74) to C-7 (δ_C 175.1). From cross peaks of H-3 (δ_H 4.83) to C-5 (δ_C 41.8), C-30 (δ_C 125.6), of H-30 (δ_H 5.39) to C-9 (δ_C 63.9), C-1 (δ_C 217.3), and of H_3-19 (δ_H 1.42) to C-1 (δ_C 217.3), C-5 (δ_C 41.8), and C-9 (δ_C 63.9), the characteristic [3, 3, 1] A/B ring system could be elucidated.[16] Furthermore, the HMBC correlations from H-17 (δ_H 5.43) to C-12 (δ_C 45.4), C-18 (δ_C 21.4), C-14 (δ_C 45.4), from H-15b (δ_H 2.73) to C-13 (δ_C 37.4), C-16 (δ_C 168.6), from H-15a (δ_H 2.85) to C-8 (δ_C 137.5), from H_3-18 (δ_H 1.11) to C-17 (δ_C 76.7), C-14 (δ_C 45.4) indicated the ring C/D in **1**.[14,16] These aforementioned data strongly suggested **1** was a B,D-*seco* mexicanolide-type limonoid,[7,19] typical constituent of *Cipadessa* genus.

Open Access Article. Published on 14 March 2018. Downloaded on 1/8/2025 8:54:51 PM.
This article is licensed under a Creative Commons Attribution-NonCommercial 3.0 Unported Licence.

Table 1 ^{1}H NMR and ^{13}C NMR spectral data of compounds **1–4** in $CDCl_3$ (δ in ppm, J in Hz)

	1[a]		**2**[a]		**3**[a]		**4**[a]	
Position	δ_H	δ_C	δ_H	δ_C	δ_H	δ_C	δ_H	δ_C
1		217.3		216.9		217.2		216.6
2	3.56, dd (8.8, 7.7)	48.9	3.50, t (9.7)	48.9	3.50[b]	49.2	3.56, t (10.0)	48.8
3	4.83, d (9.4)	77.6	4.81, d (9.5)	77.2	4.83, d (9.2)	77.3	4.83, d (9.3)	77.3
4		38.7		38.7		38.9		38.7
5	3.49, d (10.4)	41.8	3.39, dd (7.9, 3.8)	41.4	3.51[b]	40.4	3.37, d (9.5)	41.7
6	2.40, dd (16.8, 10.8)	32.2	2.38, m	33.0	2.36, dd (17.3, 10.4)	33.1	2.39, dd (17.0, 9.5)	32.8
	2.98, d (16.8)		2.38, m		2.48, d (17.3)		2.23, d (17.0)	
7		175.1		174.1		173.3		174.5
8		137.5		141.2		138.0		137.5
9	2.19, d (9.8)	63.9	2.72, dd (12.2, 5.5)	53.0	2.20[b]	56.5	2.25[b]	56.4
10		49.7		50.1		50.6		50.0
11	4.60, td (10.4, 4.6)	65.8	1.64[b]	20.2	1.73[b]	21.1	1.76, m	20.5
			2.07, dd (13.0, 4.1)		2.29, td (13.2, 3.5)		2.07, m	
12	1.39, d (11.8)	45.4	1.33, d (13.5)	28.6	1.43, td (14.0, 3.5)	34.8	1.59, m	34.2
	1.82, d (11.8)		1.98, dd (13.5, 4.1)		1.91, d (14.0)		1.83, m	
13		37.4		41.3		36.8		37.3
14	2.24, d (5.8)	45.4		73.4	2.22[b]	45.4	2.24[b]	45.4
15	2.85, dd (18.8, 5.8)	30.0	2.99, d (18.0)	39.2	2.79, m	29.2	2.80, m	29.5
	2.73, d (18.8)		2.92, d (18.0)		2.78, m		2.79, m	
16		168.6		168.6		167.8		167.0
17	5.43, s	76.7	5.66, s	77.4	5.54, s	76.6	5.73, s	78.1
18	1.11, 3H, s	21.4	1.08, 3H, s	15.9	1.00, 3H, s	22.8	1.07, 3H, s	21.9
19	1.42, 3H, s	18.7	1.16, 3H, s	15.9	1.16, 3H, s	15.7	1.16, 3H, s	15.8
20		120.5		120.1		136.1		164.1
21	7.93, s	142.4	7.84, s	142.4		168.2	4.98, dd (18.0, 2.8)	72.3
22	6.50, s	109.7	6.49, s	110.0	7.23, s	147.8	6.21, d (1.08)	118.7
23	7.45, s	143.4	7.42, s	143.0	5.80, s	102.4		172.9
28	0.83, 3H, s	22.9	0.78, 3H, s	22.5	0.79, 3H, s	22.6	0.78, 3H, s	22.5
29	0.85, 3H, s	20.3	0.82, 3H, s	20.6	0.81, 3H, s	20.9	0.82, 3H, s	20.4
30	5.39, td (7.5, 11.7)	125.6	5.63, d (6.8)	124.5	5.34, d (6.6)	123.4	5.35, d (6.9)	124.3
7-OCH_3	3.74, 3H, s	52.3	3.71, 3H, s	52.3	3.64, 3H, s	52.1	3.69, 3H, s	52.5
23- OCH_3					3.58, 3H, br s	57.6		
1′		167.2		176.7		167.3		167.1
2′		127.6	2.62, m	33.9		127.8		127.7
3′	6.90, m	139.6	1.15, 3H[b]	19.2	6.91, m	139.3	6.88, m	139.4
4′	1.80, 3H, s	11.9	1.17, 3H[b]	18.6	1.84, 3H, s	12.0	1.82, 3H, m[b]	12.0
5′	1.68, 3H, d (7.1)	14.7			1.82, 3H, d (7.3)	14.8	1.82, 3H, m[b]	14.9

[a] ^{1}H (500 MHz) NMR data of compounds. [b] Signals were overlapped.

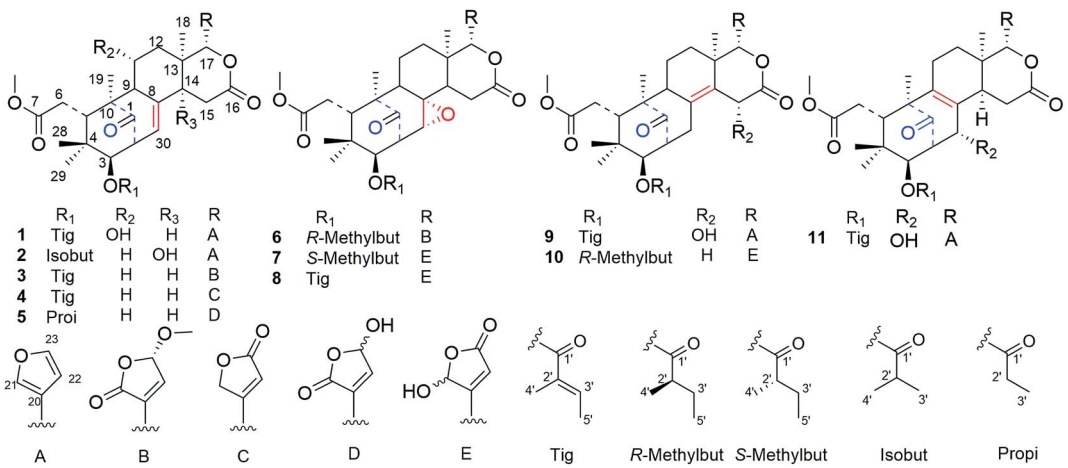

Fig. 1 Chemical structures of cipadessains A–K (**1–11**).

Open Access Article. Published on 14 March 2018. Downloaded on 1/8/2025 8:54:51 PM.
This article is licensed under a Creative Commons Attribution-NonCommercial 3.0 Unported Licence.

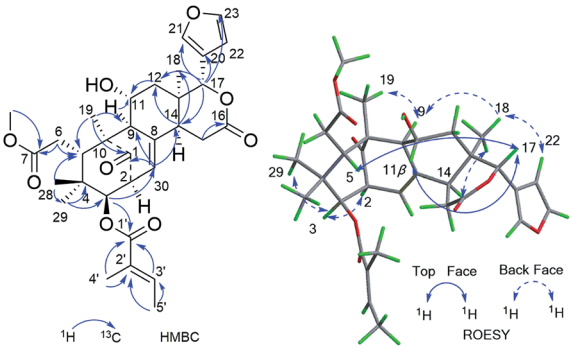

Fig. 2 Key HMBC and ROESY correlations of compound **1**.

Furthermore, the existence of $\Delta^{8,30}$ double bond was determined by the HMBC correlations from H-30 (δ_H 5.39) to C-9 (δ_C 63.9) and C-14 (δ_C 45.4), and from H-2 (δ_H 3.56) to C-1 (δ_C 217.3), C-30 (δ_C 125.6). The correlation from H-3 (δ_H 4.83) to C-1′ (δ_C 167.2) of the tigloxyl moiety [δ_H 6.90 (H-3′), 1.80 (H-4′), 1.68 (H-5′); δ_C 167.2 (C-1′), 139.6 (C-3′), 127.6 (C-2′), 14.7 (C-5′), 11.9 (C-4′)] showed the presence of a tigloxyl group at C-3. The NMR data of **1** were similar to those of 6-desoxyswietenine,[17] except for the additional of a hydroxyl group at C-11 in **1**. This inference was verified by the HSQC correlation of H-11 (δ_H 4.60) with C-11 (δ_C 65.8) and HMBC correlations from H-9 (δ_H 2.19) and H_2-12 (δ_H 1.82, 1.39) to C-11 (δ_C 65.8). Thus, the planar structure of **1** was determined as shown in Fig. 1.

The ROESY correlations between H-17 (δ_H 5.43)/H-11 (δ_H 4.60), H-5 (δ_H 3.49)/H_3-28 (δ_H 0.83) suggested these protons were the same configuration (Fig. 2). In turn, the ROESY correlations between H-2 (δ_H 3.56)/H-3 (δ_H 4.83), H-3 (δ_H 4.83)/H_3-29 (δ_H 0.85), H-14 (δ_H 2.24)/H_3-19 (δ_H 1.42) and H-9 (δ_H 2.19)/H_3-19 (δ_H 1.42) revealed that they were co-facially oriented. Accordingly, the structure of **1** was proposed as shown. Fortunately, compound **1** was recrystallized in the CH_2Cl_2/MeOH (1 : 1) mixture to yield prisms. On the basis of single-crystal X-ray diffraction data (CCDC 1815118), the absolute stereochemistry of **1** was elucidated to be 2*S*, 3*R*, 5*S*, 9*S*, 10*S*, 11*R*, 13*S*, 14*R*, 17*S* (Fig. 3). Finally, the structure of **1**, with a $\Delta^{8,30}$ double bond and a 11-hydroxyl group, was established as depicted in Fig. 1.

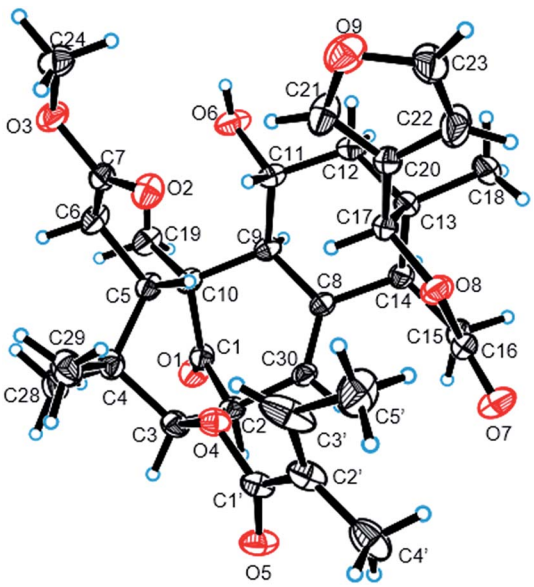

Fig. 3 Single-crystal X-ray diffraction (Cu Kα radiation) of compound **1**.

Compound **2**, was obtained as a colorless needles, which had a sodium adduct ion peak at *m*/*z* 579.2568 $[M + Na]^+$ in the HRESIMS spectrum corresponding to a molecular formula of $C_{31}H_{40}O_9$. The NMR spectroscopic data of **2** (Table 1) exhibited closed similarity to those of **1**. In comparison to **1**, the correlations from H_3-3′ (H_3-4′) to C-1′ (δ_C 176.7) and from C-2′ (δ_C 33.9), H-3 (δ_H 4.81) to C-1′ (δ_C 176.7) in the HMBC spectrum indicated the presence of an isobutyryloxyl group at C-3 in **2** instead of a tigloxyl group in **1**. An upfield shift at δ_C 20.2 (Δ − 45.6 ppm) of C-11 and a downfield shift at δ_C 73.4 (Δ + 28.0 ppm) of C-14 in the ^{13}C NMR spectrum of **2** as compared with the corresponding signals of **1** implied that the hydroxyl group was located at C-14. The deduction was supported by the HMBC correlations of C-14 (δ_C 73.4) and H_2-15 (δ_H 2.99, 2.92), H-17 (δ_H 5.66), H-30 (δ_H 5.63). The α-oriented of OH-14 was determined by comparison of NMR data of **2** with those of two known compounds Khasenegasin D and Khasenegasin E.[14] Therefore, the structure of **2** was established as shown (Fig. 1).

Compound **3** was isolated as a white amorphous powder and showed the HRESIMS ion peak at *m*/*z* 621.2669 $[M + Na]^+$ (calcd for $C_{33}H_{42}O_{10}Na$, 621.2670). The spectroscopic data of **3** were similar to those of 6-desoxyswietenine,[17] except for the presence of 23-methoxybutenolide ring moiety in **3** instead of the β-substituted furan moiety as found in 6-desoxyswietenine. This was confirmed by the HMBC correlations of OCH_3-23 (δ_H 3.58)/C-23 (δ_C 102.4); of H-23 (δ_H 5.80)/C-21 (δ_C 168.2), C-20 (δ_C 136.1); of H-22 (δ_H 7.23)/C-23 (δ_C 102.4), C-20 (δ_C 136.1), C-21 (δ_C 168.2); of H-17 (δ_C 5.54)/C-21 (δ_C 168.2), C-20 (δ_C 136.1). Thus, the planar structure of **3** was identified as shown. The relative configuration of **3** was mainly elucidated by its ROESY data and comparison of its NMR spectroscopic data with those of similar reported compounds.[17] The correlations between H-17/H-11b (δ_H 2.29), H-17/H-15b (δ_H 2.78), H-17/H-5 (δ_H 3.51), indicated these groups were on the same side of the structure, and they were assigned as β-configuration. Correlations of H_3-19 (δ_H 1.16)/H-9 (δ_H 2.20)/H-2 (δ_H 3.50), H-9/H-3 (δ_H 4.83)/H_3-29 (δ_H 0.81), H-3/H-14 (δ_H 2.22) and cross peaks of OCH_3-23/CH_3-18 revealed that these protons were α-oriented. Hence, the structure of **3** was elucidated as shown in Fig. 4 and named cipadessain C.

Compound **4**, a white, amorphous powder, displayed a molecular formula $C_{32}H_{40}O_9$, on the basis of its HRESIMS ion at *m*/*z* 591.2568 ($[M + Na]^+$, $C_{32}H_{40}O_9Na$, calcd 591.2565). The ^1H and ^{13}C NMR data (Table 1) of **3** and **4** were almost the same except for signals of the E ring. The appearance of α,β-unsaturated-γ-lactone ring portion linked to C-17 in **4** was determined by the HMBC correlations between H-17 (δ_H 5.73)/C-20 (δ_C 164.1), C-21 (δ_C 72.2), C-22 (δ_C 118.7) and H_2-21 (δ_H 4.98)/C-20 (δ_C 164.1), C-22 (δ_C 118.7), C-23 (δ_C 172.9). The ROESY correlations were observed between H-17 (δ_H 5.73)/H-5 (δ_H 3.37), H-5/H-11b (δ_H 2.07), H-5/H_3-28 (δ_H 0.78), H_3-29 (δ_H 0.82)/H-3 (δ_H 4.83), H-3/H-2 (δ_H 3.56) suggesting the relative configuration of

Open Access Article. Published on 14 March 2018. Downloaded on 1/8/2025 8:54:51 PM.
This article is licensed under a Creative Commons Attribution-NonCommercial 3.0 Unported Licence.

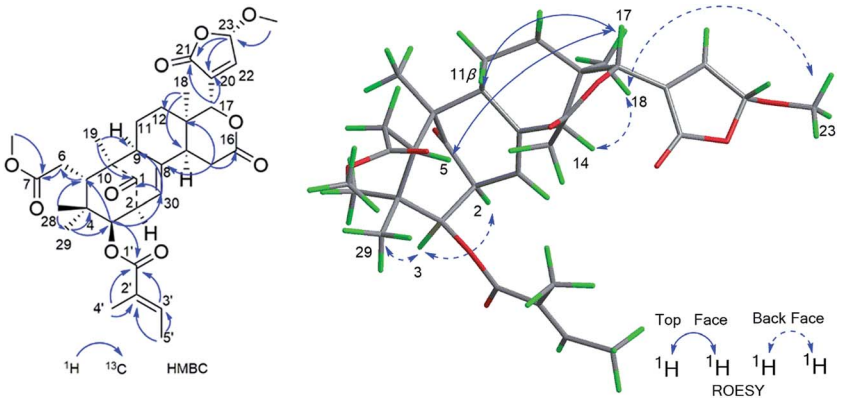

Fig. 4 Key HMBC and ROESY correlations of compound **3**.

4 was similar to that of **3**. Thus, the structure of **4** was finally determined and represented in Fig. 1.

Compound **5**, a white amorphous powder, afforded a molecular formula of $C_{30}H_{38}O_{10}$ as assigned by the (+)-HRESIMS ion peak at *m/z* 581.2353 $[M + Na]^+$ (calcd 581.2357) and the ^{13}C-NMR data. The NMR data (Table 2) of **5** resembled those of 3-de(2-methylbutanoyl)-3-propanoylcipadesin[18] except for the additional presence of 21-hydroxybutenolide unit attached to C-17 in **5**. This was confirmed by the cross peaks from H-17 (δ_H 5.60) to C-20 (δ_C 135.1/135.0), C-22 (δ_C 149.8/149.6) in the HMBC spectrum. The appearance of pairs of proton and carbon resonances in the NMR spectra of **5** indicated the presence of epimers at C-21.[19] Thus, based on these data, the planar structure of **5** was established.

Compound **6** gave a molecular formula of $C_{33}H_{44}O_{11}$ from the positive ion peak at *m/z* 639.2771 $[M + Na]^+$ (calcd for $C_{33}H_{44}O_{11}Na$, 639.2776). The 1D and 2D NMR data (Table 2) of **6** were similar to those of 2′*R*-cipadesin A,[7] a mexicanolide-type limonoid with a $\Delta^{8,30}$ epoxide ring from *Cipadessa fruticosa*. The structures **6**, featuring 23-methoxybutenolide ring in the C-17 side-chain, was verified by the key HMBC cross peaks of OCH_3-23 (δ_H 3.62/3.56)/C-23 (δ_C 103.1); H-23 (δ_H 5.82/5.78)/C-21 (δ_C 169.8), C-20 (δ_C 133.7); H-22 (δ_H 7.28)/C-17 (δ_C 76.5). In the ROESY spectrum, the cross peak of H-23 (δ_H 5.82) to H-17 (δ_H 5.10) confirmed the β-configuration of H-23 in **6**. The detailed analysis of the ROESY correlations based on the general rule,[7] in which the cross peaks of H_3-4′ (δ_H 1.25) to H-15b (δ_H 2.85) and H-30 (δ_H 3.31), of H-2′ (δ_H 2.56) to H-30 (δ_H 3.31), of H_3-5′ (δ_H 0.97) and H_3-29 (δ_H 0.79), revealed the remaining relative configurations of **6** (Fig. 5) were identical to those of 2′*R*-cipadesin A.

Compound **7**, a white amorphous powder, exhibited the molecular formula of $C_{32}H_{42}O_{11}$ based on the pseudo-molecular ion peak at *m/z* 625.2620 $[M + Na]^+$ (calcd for $C_{32}H_{42}O_{11}Na$, 625.2619). The ^{1}H and ^{13}C-NMR data of **7** were closely comparable to those of **6** for rings A–D (Table 2), while the 23-methoxybutenolide group was absent, and concomitantly a γ-hydroxylbutenolide group. This difference was supposed by the broad singlet signals of H-21 at δ_H 6.32/6.14 and H-22 at δ_H 6.34/6.22 and by carbon signals at δ_C 162.7/160.4 (C-20), 98.7/97.7 (C-21), 122.5/121.8 (C-22), 169.4/169.0 (C-23). The α-configuration of epoxide ring at C-8/C-30 was supposed from the coupling constant value of H-30 ($J = 2.5$ Hz).[20] The appearance of pairs of most proton and carbon resonances in the NMR spectra (Table 2) of **7** identified the presence of C-21 epimers. Thus, compound **7** was elucidated as a mexicanolide-type limonoid bearing γ-hydroxybutenolide group. According to the general ruler,[7] the ROESY correlations between H_3-5′ (δ_H 0.97) and H-30 (δ_H 3.30), between H-2′ (δ_H 2.55) and H-15α (δ_H 3.50), between H_3-4′ (δ_H 1.24) and H_3-29 (δ_H 0.78) confirmed its relative configurations were as the same as that of cipadesin A.

The molecular formula of **8** was determined to be $C_{32}H_{40}O_{11}$ from the HRESIMS peak at *m/z* 623.2464 (calcd for $C_{32}H_{40}O_{11}Na$, 623.2463), 2 mass units less than **7**. The NMR data of **8** (Table 2) exhibited overall similarity to those of **7**, but revealed the presence of a tigloxyl moiety instead of a 2-methylbutyryl moiety attached to C-3, this was proved by the HMBC correlations of H_3-4′ (δ_H 1.91) to C-1′ (δ_C 167.0), C-3′ (δ_C 140.6/140.2), of H_3-5′ (δ_H 1.90) to C-2′ (δ_C 127.6/127.2), of H-3 (δ_H 5.03) to C-1′ (δ_C 167.0). Therefore, the planar structure of **8** was assigned as shown. The α-configuration of epoxide ring at C8/30 was determined by the coupling constant value of H-30 ($J = 2.3$ Hz).[20] The relative configuration of the tigloxyl moiety at C-3 was β-oriented according to the observed ROESY correlations between H-3 and H-2, and the coupling constant value of H-3 ($J = 9.4$ Hz).[21] The appearance of pairs of most proton and carbon resonances in the NMR spectra (Table 2) of **8** suggested the presence of C-21 epimers. Its relative configurations were as the same as that of **7** by ROESY experiment. Therefore, the structure of **8** was elucidated as shown in Fig. 1.

The similar electronic circular dichroism spectra of **1–8** (see S1 in ESI†) indicated that the basic skeletons of these compounds possessed absolute configurations as Fig. 1.

Compound **9** was isolated as a white powder. Its molecular formula, $C_{32}H_{40}O_9$ was deduced from the HRESIMS data (*m/z* 567.2597 $[M - H]^-$, calcd for $C_{32}H_{39}O_9$, 567.2600). Analysis of its NMR spectra indicated that **9** was an analogue of procerianolide.[22] A proton signal at δ_H 4.97 was correlated with a carbon signal at δ_C 65.4 in HSQC spectrum and the HMBC correlation from the hydroxyl group (δ_H 3.18 br s) to C-15 (δ_C 65.4) indicated that the hydroxyl group was located at C-15. Furthermore, a tigloxyl moiety was located at C-3′, which was confirmed by the HMBC correlation from H-3 (δ_H 4.89) to C-

Open Access Article. Published on 14 March 2018. Downloaded on 1/8/2025 8:54:51 PM.
This article is licensed under a Creative Commons Attribution-NonCommercial 3.0 Unported Licence.

Table 2 ^{1}H NMR and ^{13}C NMR spectral data of compounds **5–8** in $CDCl_3$ (δ in ppm, J in Hz)

	5[a]		**6**[a]		**7**[a]		**8**[a]	
Position	δ_H	δ_C	δ_H	δ_C	δ_H	δ_C	δ_H	δ_C
1		217.3/217.2		214.3		213.9		214.2
2	3.49, m	48.8	3.57[b]	48.9	3.58, dd (9.5, 3.2)	48.9	3.66, d (9.3, 2.4)	49.3/49.1
3	4.75, d (9.2)	77.4[b]	5.09, d (9.2)	77.1	5.09, dd (9.5, 2.4)	77.1	5.03, d (9.3)	78.1/77.5
4		38.6		39.5		39.5/39.3		39.4/39.2
5	3.39, d (10.0)	40.7/40.7	3.21, t (5.0)	42.6	3.20, d (9.3)	42.9/42.6	3.27, d (9.4)	43.0/42.6
6	2.43, dd (17.1, 5.8)	33.1/33.0	2.35, d (5.0)	33.1	2.36	33.3	2.40, d (16.6)	33.2
	2.37[b]		2.35, d (5.0)		2.33		2.39, dd (16.6, 9.7)	
7		173.9/173.6		174.3		174.8		174.9
8		137.9/137.8		60.6		60.1		60.1
9	2.23[b]	56.3/56.2	1.90[b]	56.1	1.94[b]	54.9/54.6	1.94, m	54.8/54.4
10		50.5/50.2		48.4		48.3/48.2		48.3/48.2
11	1.73, br s	20.9	1.76, m	19.5	1.78, m	19.5	1.85, m	19.8/19.6
	2.23[b]		1.88, m		1.93[b]		2.01, m	
12	1.92, d (14.0)	34.5	1.13[b]	32.8	2.13, d (13.9)	33.1	2.10, m	33.3
	1.44, m		2.25, d (16.3)		1.39, m		1.41, m	
13		36.8/36.7		36.8		36.5/36.4		36.3/26.2
14	2.24[b]	45.5	1.49[b]	46.4	1.56, m	46.6/46.5	1.56, dd (12.7, 4.0)	46.5/46.1
15	2.84, m	29.6	3.76, m	34.7	3.50, dd (16.4, 13.7)	33.6/33.5	3.40, dd (16.1, 13.6)	33.1
	2.84, m		2.85, dd (15.5, 3.7)		2.84, dd (16.4, 4.3)		2.77, dd (16.5, 4.0)	
16		169.0/169.0		171.3		170.7		170.4
17	5.60, s	77.2	5.10, s	76.5	5.30, br s/5.15, br s	79.2/78.4	5.30, br s/5.12, br s	78.8
18	1.06/1.04, 3H, s	23.0	1.04, 3H, s	26.5	1.23/1.22, 3H, br s	16.3/16.2	1.20/1.07, 3H, br s	26.2/24.5
19	1.14, 3H, s	15.7/15.7	1.06, 3H, s	15.8	1.08/1.06, 3H, br s	26.7/26.2	1.08, 3H, br s	16.4
20		135.1/135.0		133.7		162.7		162.7/160.2
21		168.6		169.8	6.32, br s/6.14, br s	98.7/97.7	6.22, br s/6.12, br s	98.8/97.7
22	7.35/7.34, br s	149.8/149.6	7.28, s	148.8	6.33, br s/6.22, br s	122.5/121.8	6.30, br s	122.4/121.3
23	6.18/6.17, br s	97.1/96.7	5.82, br s/5.78, br s	103.1		169.4/169.0		169.1
28	0.76, 3H, s	22.5	0.81, 3H, s	21.2	0.81, 3H, s	20.9/20.9	0.83, 3H, s	23.1/23.0
29	0.79, 3H, s	21.0/20.9	0.79, 3H, s	22.5	0.78, 3H, s	22.7	0.82, 3H, s	21.0
30	5.33, d (6.5)	123.3/123.3	3.31, br s	63.7	3.30, d (2.5)	63.6/63.5	3.20, d (2.2)	63.7/63.4
7-OCH_3	3.66/3.64, 3H, br s	52.4/52.3	3.72, 3H, s	52.5				
23-OCH_3			3.62, br s/3.56, br s	57.8	3.72, 3H, s	52.8/52.6	3.74, 3H, s	52.8/52.7
1′		174.3/174.2		175.8		176.1/175.9		167.0
2′	2.39[b]	27.2/27.2	2.56, m	41.7	2.55, m	41.5/41.3		127.6/127.2
3′	1.12, d (7.5)	9.0	1.77, m	26.8	1.74, m	26.5	7.03, m	140.6/140.3
			1.54, m		1.52, m			
4′			1.25, 3H, d (7.0)	17.5	1.24, 3H, d (7.0)	17.3/17.3	1.91, 3H, m[b]	12.5
5′			0.97, 3H, t (7.4)	12.0	0.97, 3H, t (7.4)	11.9/11.8	1.90, 3H, m[b]	14.9

[a] ^{1}H (500 MHz) NMR data of compounds. [b] Signals were overlapped.

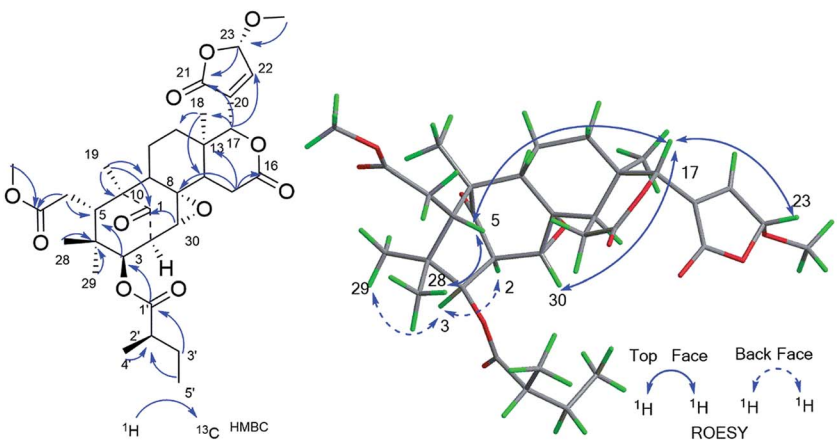

Fig. 5 Key HMBC and ROESY correlations of compound **6**.

Open Access Article. Published on 14 March 2018. Downloaded on 1/8/2025 8:54:51 PM.
This article is licensed under a Creative Commons Attribution-NonCommercial 3.0 Unported Licence.

1′ (δ_C 167.2). In the ROESY spectrum, the H-15 (δ_H 4.97) was correlated with H-17 (δ_H 5.54), which suggested the H-15 was β-oriented. The other configurations of **9** were similar to that of proceranolide by ROESY spectroscopic analysis.

Compound **10**, was isolated as a white powder and its molecular formula $C_{32}H_{42}O_{10}$ was determined by the molecular ion peak at *m/z* 609.2675 (calcd for $C_{32}H_{42}O_{10}Na$, 609.2670) in the HRESIMS. The 1D and 2D NMR data indicated that **10** was also a mexicanolide-type limonoid bearing a γ-hydroxylbutenolide unit as **8**. A comparison of their NMR data (Table 3) revealed the main differences being the presence of the $\Delta^{8,14}$ double bond and the absence of the $\Delta^{8,30}$ epoxide ring. The conclusion was confirmed from the HMBC correlations of H-15b (δ_H 3.46) to C-8 (δ_C 129.2/128.9), of H-30b (δ_H 2.12) to C-14 (δ_C 130.8/130.5), of H-2 (δ_H 3.19) to C-8 (δ_C 129.2/128.9). Moreover, the tigolxyl group was replaced by the *R*-methylbutyryl at C-3 in **10**, which can be proved from the H-3 (δ_H 4.97) to C-1′ (δ_C 176.3). The appearance of pairs of proton and carbon resonances in the NMR spectra of **10** indicated that the presence of epimers at C-21. Therefore, the structure of **10** was shown in Fig. 1. The relative structure of **10** was displayed by the ROESY experiment and general ruler.[7]

Compound **11**, was isolated as white and amorphous powder, shown as a positive HRESIMS ion peak at *m/z* 591.2562 ($[M + Na]^+$, calcd for $C_{32}H_{40}O_9Na$ 591.2565). The ^1H and ^{13}C-NMR data of **11** (Table 3) suggested that its structure was closely related to that of khasengasin N with $\Delta^{8,9}$ double bond.[14] The only difference between **11** and khasengasin N was that a hydroxyl group linked to C-3 as found in khasengasin N was replaced by a tigloxyl group [δ_H 1.89 (s), δ_H 1.86 (d, $J = 7.1$ Hz) and 6.92 (m)] in **11**. Further, it was evidenced by HMBC correlation of H-3 (δ_H 5.17) to C-1′ (δ_C 167.0) of the tigloxyl group. The relative configuration of **11** was assigned by the ROESY

Table 3 ^1H NMR and ^{13}C NMR spectral data of compounds **9–11** in $CDCl_3$ (δ in ppm, J in Hz)

	9[a]		**10**[b]		**11**[a]	
Position	δ_H	δ_C	δ_H	δ_C	δ_H	δ_C
1		217.7		217.5/217.3		213.4
2	3.26, m	48.4	3.19, m	48.1	3.19, dd (7.9, 1.9)	57.0
3	4.89, m	79.3	4.97, d (9.8)	78.0/77.9	5.17, d (7.9)	77.1
4		38.8		38.4/38.2		38.4
5	3.37, dd (11.0, 1.5)	40.7	3.11, d (10.7)	41.4/41.2	2.83, t (6.0)	48.4
6	2.42, d (16.5, 11.0)	33.4	2.45, m	33.9	2.29, d (6.0)	32.4
	2.37, d (16.5)		2.36, m			
7		174.7		176.3/175.7		174.1
8		135.7		129.2/128.9		130.7
9	2.11, d (6.6)	51.9	2.05[c]	51.3		142.1
10		53.6		53.1/52.8		50.9
11	1.75, m	18.7	1.79, m	18.7/18.6	2.03, m	21.6
	1.89, m		1.94, m		2.38, m	
12	1.00	28.6	1.99, m	28.6	1.58[c]	29.1
	1.78, m		1.27, m		1.51[c]	
13	1.02, m	38.8		39.1		35.8
14		135.0		130.8/130.5	2.45[c]	38.2
15	4.97, s	65.4	3.77, m	32.9	2.80, dd (14.0, 3.0)	31.4
			3.46, d (21.0)		2.41, d (14.0)	
16		174.5		168.7/168.1		172.7
17	5.54, s	81.9	5.62, br s/5.35, br s	79.7	4.91, s	81.3
18	1.02, 3H, s	16.9	1.08, 3H, s	17.4	0.74, 3H, s	20.4
19	1.18, 3H, s	16.7	1.17, 3H, s	16.9	1.08, 3H, s	17.2
20		120.6		162.8		120.8
21	7.62, s	142.0	6.10, s	98.9/98.0	7.43, s	140.5
22	6.51, s	110.0	6.30, s	122.8/122.1	6.40, s	109.8
23	7.42, s	143.0		169.6/159.4	7.43, s	143.4
28	0.76, 3H, s	20.4	0.68, 3H, s	23.5	1.14, 3H, s	26.5
29	0.83, 3H, s	23.9	0.81, 3H, s	20.6	0.89, 3H, s	25.9[c]
30	2.99,dd, (15.9, 1.9)	34.6	2.72, d (15.0)	33.1	4.54, br s	71.4
	2.30, dd, (15.9, 6.6)		2.12, d (6.0)			
7-OCH_3	3.73, 3H, s	52.6	3.71, 3H, s	52.8/52.2	3.69, 3H, s	52.2
15-OH	3.18, br s					
1′		167.2		176.3		167.0
2′		129.4	2.40, m	41.3		128.5
3′	6.90, m	138.6	1.73, dt (20.0, 7.0)	27.3	6.92, m	139.1
			1.51, dt (14.0, 7.0)			
4′	1.87, 3H, m	12.5	1.21, 3H, m	16.2	1.89, 3H, s	12.5
5′	1.79, 3H, d (7.0)	14.6	0.91, 3H, dd (7.1, 5.5)	11.3	1.86, 3H, d (7.1)	14.9

[a] ^1H (500 MHz) NMR data of compounds. [b] ^1H (600 MHz) NMR data of compound. [c] Signals were overlapped.

Open Access Article. Published on 14 March 2018. Downloaded on 1/8/2025 8:54:51 PM.
This article is licensed under a Creative Commons Attribution-NonCommercial 3.0 Unported Licence.

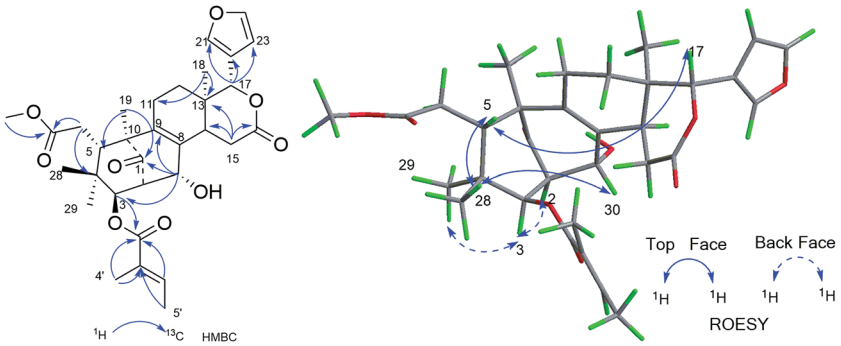

Fig. 6 Key HMBC and ROESY correlations of compound **11**.

Table 4 Cytotoxicity and NO inhibition activities of compounds **1–11**[a,b]

Compounds	NO inhibition RAW 264.7 macrophages	Cytotoxicity (HepG2)
3	5.79 ± 0.18	5.23 ± 0.12
4	23.90 ± 2.1	>50
6	6.93 ± 0.89	8.67 ± 1.02
7	20.54 ± 0.63	>50
L-NMMA[c]	41.88 ± 0.91	—
Doxorubicin[c]	—	1.04 ± 0.37

[a] Values were expressed as the means ± SD based on three independent experiments. [b] Compounds **1,2,5,8–11** were inactive. [c] Positive controls.

experiment, in which key cross-peaks between H-17/H-5, H-5/H-30 indicated H-30 to be β-oriented (Fig. 6). Therefore, the structure of **11** was demonstrated as shown in Fig. 1.

All the isolates were evaluated for their cytotoxicity against HepG2 cancer cell line with doxorubicin as the positive control. As shown in Table 4, compounds **3** and **6** showed significant cytotoxic activities. These isolates were further tested for their inhibitory effects on NO production of LPS-activated RAW 264.7 macrophages with *N*-monomethyl-L-arginine as the positive control (IC_{50} 41.88 ± 0.91 μM). The results showed that compounds **3** and **6** exhibited significant NO inhibitory activities with IC_{50} values of 5.79 ± 0.18 μM, 6.93 ± 0.89 μM, respectively. On the contrary, those mexicanolides bearing complete furan moiety or hydroxybutenolide furan moiety were inactive (**1**, **2**, **5**, **8–11**). According to the continuing study,[14–16] the modified furan moiety may play important role on the bioactivity of these limonoids.

Conclusions

In summary, eleven new mexicanolide-type limonoids, cipadessains A–K (**1–11**) were isolated from the fruits of *Cipadessa cinerascens*. Their structures were elucidated on the NMR data and HRESIMS. The absolute configuration of **1** was determined by X-ray diffraction. In bioactivity screening, two mexicanolides (**3** and **6**) bearing methoxybutenolide moiety originated from the furan ring showed significant cytotoxicity activities against HepG2 cell line and NO inhibitory activities in LPS-activated RAW 264.7 macrophages, which were more excellent than those limonoids with complete furan moiety or hydroxybutenolide furan moiety. This finding adds the complexity and diversity of mexicanolide-type limonoids in *Cipadessa cinerascens*. It's worthy of paying more attention to the cytotoxicity activities against HepG2 cell line of the limonoids with modified furan rings from the *Cipadessa* genus.

Experimental

General experimental procedures

UV and IR were recorded on a Shimadzu UV-2450 spectrophotometer (Shimadzu, Tokyo, Japan) and Bruker Tensor 27 spectrometer (Bruker, Karlsruhe, Germany), optical rotations were measured on a JASCO P-1020 polarimeter (Jasco, Tokyo, Japan). ECD spectra were obtained on a JASCO J-810 spectropolarimeter (Jasco, Tokyo, Japan) respectively. 1D and 2D NMR spectra were measured by a Bruker AVIII-600 and AVIII-500 NMR instrument at 600 and 500 MHz (^{1}H), 150 MHz (^{13}C) and 125 MHz (^{13}C) in $CDCl_3$. HRESI mass spectra were conducted on an Agilent 6520B UPLC-Q-TOF mass spectrometer (Agilent Technologies, Santa Clara, CA, USA). MCI gel (Mitsubishi Chemical Corp., Tokyo, Japan), MPLC (Beijing H&E Co., Ltd., Beijing, China), and RP-C_{18} (40–63 μm, FuJi), silica gel (Qingdao Haiyang Chemical Co., Ltd.) were used as column chromatography. Preparative HPLC was performed on a Shimadzu LC-6AD instrument with a SPD-10A detector using a shim-pack reversed-phase C_{18} column (20 × 200 mm, 10 μm). Analytical HPLC was carried out on an Agilent 1260 Series instrument with a DAD detector using a shim-pack VP-ODS column (250 × 4.6 mm, 5 μm). All solvents used were analytical grade (Jiangsu Hanbon Science and Technology Co., Ltd.). The mouse macrophage cell line RAW264.7 and human hepatocellular carcinoma (HepG2) cell were obtained from the Cell Bank of the Shanghai Institute of Cell Biology and Biochemistry, Chinese Academy of Sciences (Shanghai, China). All cells were cultured in Dulbecco's modified Eagle medium (DMEM, GIBCO Invitrogen Corp., Carlsbad, CA, USA) with 10% FBS, penicillin (100 U ml^{-1}), and streptomycin (100 μg ml^{-1}) in a humidified atmosphere with 5% CO_2 at 37 °C.

Plant material

The air-dried fruits of *Cipadessa cinerascens* (Pellegr) Hand.-Mazz (Meliaceae) were collected from Xishuangbanna,

Open Access Article. Published on 14 March 2018. Downloaded on 1/8/2025 8:54:51 PM. This article is licensed under a Creative Commons Attribution-NonCommercial 3.0 Unported Licence.

Yunnan province, People's Republic of China, in July 2013, and authenticated by Professor Mian Zhang, Research Department of Pharmacognosy, China Pharmaceutical University. A voucher specimen (no. 2015-CCHM) has been deposited in the Department of Natural Medicinal Chemistry, China Pharmaceutical University.

Extraction and isolation

The dried and powdered fruits of *Cipadessa cinerascens* (5.0 kg) were extracted by refluxing with 95% ethanol (25 L × 4), for 4 h, 4 h, 4 h, 3 h. The ethanol extract was concentrated under reduced pressure to afford the crude extract (637 g), it was suspended in H_2O (1.5 L) and partitioned sequentially with petroleum ether (PE), CH_2Cl_2, EtOAc. The oily PE and CH_2Cl_2 part were subjected to a silica gel column gradient eluted with CH_2Cl_2/MeOH (150 : 1 to 0 : 100) to afford collect six fractions A–F by TLC analysis. Fraction C (120 g) was run on a D101-macroporous absorption resin, eluted with EtOH/H_2O (30%, 50%, 70%, and 90%, v/v) to give six sub-fractions (C_1–C_6) monitored by HPLC. Fr. C_3 (12.8 g) was chromatographed on an ODS-C_{18} column eluted with MeOH/H_2O (30 : 70 to 100 : 0) to obtain fourteen sub-fractions (C_3A–C_3N). Fraction C_3A was subjected to an ODS-C_{18} column eluted with MeOH/H_2O (40 : 60, v/v) to obtain ten sub-fractions (C_3A_1–C_3A_{10}). C_3A_5 was purified by semi-preparative HPLC yielding **5** (2.2 mg). Fraction C_3F was applied to a silica gel column (CH_2Cl_2/MeOH; 100 : 1 to 0 : 100) to give five sub-fractions (C_3F_1–C_3F_5). Fraction C_3F_2 (102 mg) was separated by the semi-preparative HPLC (MeOH/H_2O; 65 : 35, v/v, 10 mL min^{-1}) to yield **3** (5.2 mg). Using the same purification procedures, fraction C_3E yielded **4** (2.3 mg), **7** (2.1 mg) and **10** (8.6 mg). Fraction C_3I was subjected to a Sephadex LH-20 gel, using CH_2Cl_2/MeOH (1 : 1) as the eluent, to obtain three sub-fractions, C_3I_1–C_3I_3. C_3I_2 was separated by the semi-preparative HPLC (MeOH/H_2O; 65 : 35, v/v, 10 ml min^{-1}) to obtain **8** (1.8 mg). Fraction C_3K (2.01 g) was subjected to MPLC to give six sub-fractions (C_3K_1–C_3K_6). Fraction C_3K_1 was repeatedly chromatographed over semi-preparative HPLC (MeCN/H_2O; 50 : 50, v/v, 10 ml min^{-1}) to afford **1** (2.2 mg), **2** (2.0 mg), **9** (4.5 mg), **11** (4.3 mg) in turn. Fraction C_3K_3 (350 mg) was subjected to silica gel column (CH_2Cl_2/MeOH; 100 : 1 to 0 : 100), further purified by the semi-preparative HPLC (MeCN/H_2O; 55 : 45) to obtain **6** (1.8 mg).

Cipadessain A (1). Colorless crystals (MeOH : CH_2Cl_2 = 1 : 1); $[\alpha]_D^{25}$ −47.6 (*c* 0.10, MeOH); UV (MeOH) λ_{max} (log ε) 229 (3.58) nm; ECD (MeOH, $\Delta\varepsilon$) 200 (−14.074), 239 (+1.894), 294 (−4.559) nm; IR (KBr) ν_{max} 3451, 2922, 1640, 1384 cm^{-1}; ^1H and ^{13}C NMR data, see Table 1; HRESIMS *m/z* 591.2560 $[M + Na]^+$ (cacld for $C_{32}H_{40}O_9Na$, 579.2565).

Cipadessain B (2). Colorless crystals (MeOH : CH_2Cl_2 = 1 : 1); $[\alpha]_D^{25}$ −119.3 (*c* 0.13, MeOH); UV (MeOH) λ_{max} (log ε) 227 (3.58) nm; ECD (MeOH, $\Delta\varepsilon$) 200 (−11.079), 212 (+4.854), 293 (−2.852) nm; IR (KBr) ν_{max} 3452, 1730, 1640, 1384 cm^{-1}; ^1H and ^{13}C NMR data, see Table 1; HRESIMS *m/z* 579.2568 $[M + Na]^+$ (cacld for $C_{31}H_{40}O_9Na$, 579.2565).

Cipadessain C (3). White powder; $[\alpha]_D^{25}$ −44.6 (*c* 0.13, MeOH); UV (MeOH) λ_{max} (log ε) 210 (3.91) nm; ECD (MeOH, $\Delta\varepsilon$) 200 (−43.442), 229 (+5.615), 294 (−5.617) nm; IR (KBr) ν_{max} 3453, 1727, 1647, 1437, 1383, 1263 cm^{-1}; ^1H and ^{13}C NMR data, see Table 1; HRESIMS *m/z* 621.2669 $[M + Na]^+$ (calcd for $C_{33}H_{42}O_{10}Na$, 621.2670).

Cipadessain D (4). White powder; $[\alpha]_D^{25}$ −79.1 (*c* 0.13, MeOH); UV(MeOH) λ_{max} (log ε) 234 (3.47) nm; ECD (MeOH, $\Delta\varepsilon$) 200 (−13.199), 255 (+0.468), 294 (−3.856) nm; IR (KBr) ν_{max} 3455, 1726, 1643, 1455 cm^{-1}; ^1H and ^{13}C NMR data, see Table 1; HRESIMS *m/z* 591.2568 $[M + Na]^+$ (calcd for $C_{32}H_{40}O_9Na$, 591.2565).

Cipadessain E (5). White powder; $[\alpha]_D^{25}$ −56.8 (*c* 0.10, MeOH); UV (MeOH) λ_{max} (log ε) 208 (3.61) nm; ECD (MeOH, $\Delta\varepsilon$) 200 (−22.845), 224 (+7.992), 297 (−5.732) nm; IR (KBr) ν_{max} 3455, 1726, 1643, 1455 cm^{-1}; ^1H and ^{13}C NMR data, see Table 1; HRESIMS *m/z* 581.2353 $[M + Na]^+$ (calcd for $C_{31}H_{38}O_8Na$, 581.2357).

Cipadessain F (6). White powder; $[\alpha]_D^{25}$ −34.0 (*c* 0.09, MeOH); UV (MeOH) λ_{max} (log ε) 219 (3.64) nm; ECD (MeOH, $\Delta\varepsilon$) 200 (−4.342), 252 (+1.559), 296 (−3.587) nm; IR (KBr) ν_{max} 3451, 1639, 1384, 617 cm^{-1}; ^1H and ^{13}C NMR data, see Table 2; HRESIMS *m/z* 639.2771 $[M + Na]^+$ (calcd for $C_{33}H_{44}O_{11}Na$, 639.2771).

Cipadessain G (7). White powder; $[\alpha]_D^{25}$ −40.1 (*c* 0.10, MeOH); UV (MeOH) λ_{max} (log ε) 210 (3.86) nm; ECD (MeOH, $\Delta\varepsilon$) 209 (−11.148) 246 (+4.267), 294 (−6.172) nm; IR (KBr) ν_{max} 3460, 2969, 1768, 1635, 1460 cm^{-1}; ^1H and ^{13}C NMR data, see Table 2; HRESIMS *m/z* 625.2620 $[M + Na]^+$ (calcd for $C_{32}H_{42}O_{11}Na$, 625.2619).

Cipadessain H (8). White, amorphous powder; $[\alpha]_D^{25}$ −54.9 (*c* 0.10, MeOH); UV (MeOH) λ_{max} (log ε) 230 (3.35) nm; ECD (MeOH, $\Delta\varepsilon$) 200 (−16.272), 224 (+7.992), 297 (−5.732); IR (KBr) ν_{max} 3451, 2969, 1768, 1641, 1457 cm^{-1}; ^1H and ^{13}C NMR data, see Table 2; HRESIMS *m/z* 623.2463 $[M + Na]^+$ (calcd for $C_{32}H_{40}O_{11}Na$, 623.2464).

Cipadessain J (9). White powder; $[\alpha]_D^{25}$ −108.41 (*c* 0.10, MeOH); UV (MeOH) λ_{max} (log ε) 213 (3.80) nm; ECD (MeOH, $\Delta\varepsilon$) 200 (−20.403), 222 (+15.345) nm; IR (KBr) ν_{max} 3400 1725, 1645, 1460 cm^{-1}; ^1H and ^{13}C NMR data, see Table 3; HRESIMS *m/z* 567.2597 $[M - H]^-$ (cacld for $C_{32}H_{39}O_9Na$, 567.2600).

Cipadessain I (10). White powder; $[\alpha]_D^{25}$ −33.1 (*c* 0.10, MeOH); UV (MeOH) λ_{max} (log ε) 228 (4.14) nm; ECD (MeOH, $\Delta\varepsilon$) 200 (−5.196), 208 (+2.013), 225 (−5.931), 258 (+8.547), 296 (−11.285) nm; IR (KBr) ν_{max} 3445, 1730, 1643, 1142 cm^{-1}; ^1H and ^{13}C NMR data, see Table 3; HRESIMS *m/z* 609.2675 $[M + Na]^+$ (calcd for $C_{32}H_{42}O_{10}Na$, 609.2670).

Cipadessain K (11). Colorless needles (MeOH–H_2O); $[\alpha]_D^{25}$ −41.5 (*c* 0.10, MeOH); UV (MeOH) λ_{max} (log ε) 229 (3.48) nm; ECD (MeOH, $\Delta\varepsilon$) 200 (+12.576), 294 (−3.937) nm; IR (KBr) ν_{max} 3460, 2931, 1728, 1648 cm^{-1}; ^1H and ^{13}C NMR, see Table 3; HRESIMS *m/z* 591.2565 $[M + Na]^+$ (cacld for $C_{32}H_{40}O_9Na$, 579.2565).

X-ray crystallographic analysis of 1. Colorless crystals of **1** were recrystallized from CH_2Cl_2–MeOH (1 : 1). Crystal data were obtained on a Bruker Smart-1000 CCD with a graphite monochromator with Cu Kα radiation (λ = 1.54184 Å) at 290(2) K. The structure was solved by direct methods using the SHELXS-97 (ref. 23) and expanded with difference Fourier techniques, refined with the SHELXL-97.[24]

Open Access Article. Published on 14 March 2018. Downloaded on 1/8/2025 8:54:51 PM.
This article is licensed under a Creative Commons Attribution-NonCommercial 3.0 Unported Licence.

Crystal data of 1. $C_{32}H_{40}O_9$ ($M = 568.64$); monoclinic crystal ($0.280 \times 0.250 \times 0.200$ mm^3); space group $P2_12_12_1$; unit cell dimensions $a = 1.49100$ (10) Å, $b = 13.49460$ (10) Å, $c = 18.7471$ (2) Å, $V = 2907.05$ (5) Å^3, $Z = 4$, $T = 290$ (2) K, μ (Cu Kα) = 0.776 mm^{-1}, Dcalc = 1.299 g cm^{-3}, 26 163 reflections measured ($8.072° \leq 2\Theta \leq 142.798°$), 5564 unique ($R_{int} = 0.0242$, $R_{sigma} = 0.0160$) which were used in all calculations. The final R_1 was 0.0420 ($I > 2\sigma$ (I)) and wR_2 was 0.1182 (all data). Flack parameter = −0.03 (5).

Anti-inflammatory activities

All new compounds were evaluated for their inhibitory effects on NO production in lipopolysaccharide-activated RAW 264.7 macrophages as described in the literature.[25] L-NMMA were used as positive control. All experiments were conducted for three independent replicates.

In vitro cytotoxicity assay

All new compounds were evaluated for their cytotoxicities against $HepG_2$ by MTT assay.[26] Cells were plated in 96-well culture plates (5×103 cells per well). After incubation overnight, the cells were treated with different concentrations of each compound for 48 h. DMSO (0.1%) was used as a vehicle. MTT (5 mg mL^{-1}) was dissolved in PBS and filter sterilized, then 20 μL of the prepared solution was added to each well and cells were incubated until a purple precipitate was visible. The formed formazan crystals were dissolved in DMSO (150 μL per well) by constant shaking for 10 min. The absorbance was measured on an ELISA reader (SpectraMax Plus = 384, Molecular Devices, Sunnyvale, CA) at a test wavelength of 570 nm and a reference wavelength of 630 nm. After treatment, cell viability was detected and IC_{50} values were calculated by the Reed and Muench method.[26] All experiments were performed as three independent replicates.

Conflicts of interest

The authors declare no conflict of interest.

Acknowledgements

This research work was financially supported by the National Natural Science Foundation of China (31470416), the Outstanding Youth Fund of the Basic Research Program of Jiangsu Province (BK20160077), the PhD Programs Foundation of Ministry of Education of China (20120096130002), the Program for Changjiang Scholars and Innovative Research Team in University (IRT_15R63), and the Priority Academic Program Development of Jiangsu Higher Education Institutions (PAPD).

References

1 S. K. Chen, B. Y. Chen and H. Li in *Zhongguo Zhiwu Zhi*, Science Press, BeiJing, 1997, vol. 43, p. 58.
2 S. G. Liao, H. D. Chen and J. M. Yue, *Chem. Rev.*, 2009, **109**, 1092–1140.
3 Q. G. Tan and X. D. Luo, *Chem. Rev.*, 2011, **111**, 7437–7522.
4 A. K. R. Bandi and D. U. Lee, *Chem. Biodiversity*, 2012, **9**, 1403–1421.
5 B. Siva, B. Poominma, A. Venkanna, K. Rajendra Prasad, B. Sridhar, V. Lakshma Nayak, S. Ramakrishna and K. Suresh Babu, *Phytochemistry*, 2014, **98**, 174–182.
6 X. Fang, Y. T. Di, C. S. Li, Z. L. Geng, Z. Zhang, Y. Zhang, S. Y. Yang and X. J. Hao, *J. Nat. Prod.*, 2009, **72**, 714–718.
7 L. S. Gan, X. N. Wang, Y. Wu and J. M. Yue, *J. Nat. Prod.*, 2007, **70**, 1344–1347.
8 Y. T. Di, P. H. He, H. Y. Liu, P. Yi, Z. Zhang, Y. L. Ren, J. S. Wang, F. W. Yang, X. Fang, S. l. Li, H. J. Zhu and X. J. Hao, *J. Nat. Prod.*, 2007, **70**, 1352–1355.
9 L. G. Lin, C. P. Tang, C. Q. Ke, Y. Zhang and Y. Ye, *J. Nat. Prod.*, 2008, **71**, 628–632.
10 X. Fang, Q. Zhang, C. J. Tan, S. Z. Mu, Y. Lü, Y. B. Lu, Q. T. Zheng, Y. T. Di and X. J. Hao, *Tetrahedron*, 2009, **65**, 7408–7414.
11 H. J. Yu, Q. F. Liu, L. Sheng, G. C. Wang and J. M. Yue, *Org. Lett.*, 2016, **18**, 444–447.
12 X. Fang, Y. T. Di, G. W. Hu, S. L. Li and X. J. Hao, *Biochem. Syst. Ecol.*, 2009, **37**, 528–530.
13 J. Ning, Y. T. Di, X. Fang, H. P. He, Y. Y. Wang, Y. Li, S. L. Li and X. J. Hao, *J. Nat. Prod.*, 2010, **73**, 1327–1331.
14 H. Li, Y. Li, X. B. Wang, T. Pang, L. Y. Zhang, J. Luo and L. Y. Kong, *RSC Adv.*, 2015, **5**, 40465–40474.
15 X. M. Tian, H. Li, F. An, R. J. Li, M. M. Zhou, M. H. Yang, L. Y. Kong and J. Luo, *Planta Med.*, 2017, **83**, 341–350.
16 Y. Li, Q. Lu, J. Luo, J. S. Wang, X. B. Wang, M. D. Zhu and L. Y. Kong, *Chem. Pharm. Bull.*, 2015, **63**, 305–310.
17 T. R. Govindachari, B. Banumathy, G. Gopalakrishnan and G. Suresh, *Fitoterapia*, 1991, **70**, 106–108.
18 X. Y. Wang, C. M. Yuan, G. H. Tang, T. Zou, F. Guo, J. H. Liao, H. Y. Zhang, G. Y. Zuo, G. X. Rao, Q. Zhao, X. J. Hao and H. P. He, *J. Asian Nat. Prod. Res.*, 2014, **16**, 795–799.
19 M. Y. Li, X. B. Yang, J. Y. Pan, G. Feng, Q. Xiao, J. Sinkkonen, T. Satyanandamurty and J. Wu, *J. Nat. Prod.*, 2009, **72**, 2110–2114.
20 A. C. Leite, J. B. Fernandes, M. Fatima das and G. F. da Silva, *Z. Naturforsch. B*, 2005, **60**, 351–355.
21 K. L. Mikolajczak, D. Weisleder, L. Parkanyi and J. Cladry, *J. Nat. Prod.*, 1988, **51**, 606–610.
22 B. L. Sondengam, C. S. Kamga and J. D. Connolly, *Phytochemistry*, 1980, **19**, 2488.
23 G. M. Sheldrick, SHELXS-97, *Program for Crystal Structure Resolution*, University of Göttingen, Germany, 1997.
24 G. M. Sheldrick, SHELXL-97, *Program for Crystal Structure Refinement*, University of Göttingen, Germany, 1997.
25 Y. S. Li, M. Ishibashi, M. Satake, X. G. Chen, Y. Oshima and Y. Ohizumi, *J. Nat. Prod.*, 2003, **66**, 696–698.
26 L. J. Reed and H. A. Muench, *Am. J. Hyg.*, 1938, **27**, 493–497.